

Research Article

Tetrastigma hemsleyanum Vine Flavone Ameliorates Glutamic Acid-Induced Neurotoxicity via MAPK Pathways

Qiang Chu,^{1,2} Yonglu Li,² Zheng Hua,² Yaxuan Wang,² Xin Yu,² Ruoyi Jia,² Wen Chen,² and Xiaodong Zheng² 

¹State Key Laboratory of Silicon Materials, School of Materials Science and Engineering, Zhejiang University, Hangzhou 310027, China

²Department of Food Science and Nutrition, National Engineering Laboratory of Intelligent Food Technology and Equipment, National-Local Joint Engineering Laboratory of Intelligent Food Technology and Equipment, Key Laboratory for Agro-Products Postharvest Handling of Ministry of Agriculture, Zhejiang Key Laboratory for Agro-food Processing, Fuli Institute of Food Science, Zhejiang University, Hangzhou 310058, China

Correspondence should be addressed to Xiaodong Zheng; xdzhengzju@163.com

Received 4 February 2020; Accepted 21 February 2020; Published 22 March 2020

Guest Editor: Francisco Jaime B. Mendonça Junior

Copyright © 2020 Qiang Chu et al. This is an open access article distributed under the Creative Commons Attribution License, which permits unrestricted use, distribution, and reproduction in any medium, provided the original work is properly cited.

Glutamic acid (Glu) is a worldwide flavor enhancer with various positive effects. However, Glu-induced neurotoxicity has been reported less. *Tetrastigma hemsleyanum* (TH), a rare herbal plant in China, possesses high medicinal value. More studies paid attention to tuber of TH whereas vine part (THV) attracts fewer focus. In this study, we extracted and purified flavones from THV (THVF), and UPLC-TOF/MS showed THVF was consisted of 3-caffeoylquinic acid, 5-caffeoylquinic acid, quercetin-3-O-rutinoside, and kaempferol-3-O-rutinoside. *In vitro*, Glu caused severe cytotoxicity, genotoxicity, mitochondrial dysfunction, and oxidative damage to rat pheochromocytoma (PC12) cells. Conversely, THVF attenuated Glu-induced toxicity via MAPK pathways. *In vivo*, the neurotoxicity triggered by Glu restrained the athletic ability in *Caenorhabditis elegans* (*C. elegans*). The treatment of THVF reversed the situation induced by Glu. In a word, Glu could cause neurotoxicity and THVF owns potential neuroprotective effects both *in vitro* and *in vivo* via MAPK pathways.

1. Introduction

Glutamic acid (Glu), as one of the basic amino acids, is widely applied in industry. Glu is involved in many crucial chemical reactions in the body and plays an important role in protein metabolism in organisms [1]. Meanwhile, it is ubiquitous in the human diet; as a flavor enhancer and food additive in food field, Glu is widely used to improve the taste of beverages and foods and preserves the freshness of animal food [2, 3]. For example, sodium glutamate, commonly known as monosodium glutamate, is a typical flavor agent that can be used alone or with other amino acids [4]. In addition, studies have proven that Glu is an excellent hair-generating agent. Ottersen et al. reported that Glu effectively promoted the proliferation of hair papilla cells; besides, it can also expand blood vessels and accelerated blood circulation,

resulting in hair regeneration [5, 6]. It has also been estimated that Glu poses the ability to reduce wrinkles [7]. As an auxiliary drug for liver diseases, Glu is taken and combined with blood ammonia to form glutamine, which can relieve the toxic effect of ammonia in the metabolic process, thus preventing and treating hepatic coma [8, 9]. Besides, brain tissue cannot oxidize amino acids except glutamate, and therefore, glutamine can be used as an energy substance to improve the function of the brain [10, 11]. As a supplement to the nerve center and cerebral cortex, Glu exhibits a certain effect on the treatment of concussion, nerve damage, epilepsy, and mental retardation [12, 13]. Data show that Glu peaks the largest productive amino acid variety worldwide.

Although Glu shows an irreplaceable role in various fields, it may also turn from a protective agent to a neurotoxin in many cases. A growing number of studies have

found that the Glu is closely associated with the etiology and pathology of many neurological and psychiatric disorders, such as cerebral ischemia, epilepsy, Alzheimer's disease, Huntington's disease, schizophrenia, and Pico disease [14]. Oxidative stress caused by Glu is an important cause of neurodegenerative diseases [15, 16], high concentration of Glu inhibits cysteine/glutamate antiporter or system x-CT in neuronal cells, causes calcium overload that interferes with mitochondrial respiratory chain function, thereby inhibiting cysteine uptake and causing intracellular glutathione (GSH) deprivation and ROS accumulation, and ultimately leading to cell necrosis or apoptosis [17, 18]. Moreover, studies have shown that the caspase-dependent apoptotic pathway is related with Glu-neurotoxicity [19].

Natural plant extracts are attracting researchers' attention because of their safety, nontoxicity, and various biological activities [20]. Many natural plants have been already proved to exhibit various bioactive capacities such as antioxidative activity, anti-inflammatory activity, hypolipidemic effects, and even antitumor capacity [20]. *Tetragium hemsleyanum* Diels et. Gilg (TH), initially used for folk treatment of cancer (Li et al., 2019), is now not only a traditional Chinese medicine but also a type of functional food. Previous studies have shown that TH has antioxidant, anti-inflammatory, anticancer, and immunomodulatory properties that can effectively treat high fever, infantile febrile seizures, pneumonia, asthma, hepatitis, rheumatism, menstrual disorders, sore throats, and sores [21, 22]. It has reported that TH contains many phytochemicals, such as flavonoids, phenolic acids, polysaccharides, and phytosterols, resulting in its various biological activities such as anti-inflammatory, antioxidant, antiproliferative, antitumor, and antiviral effects [22–24]. However, there are fewer studies that paid attention to vine of TH, which is usually regarded useless and often discarded as a by-product, resulting in a waste of source.

In this study, we have extracted and purified the THVF, then identified and characterized the main compounds of THVF by UPLC-TOF/MS. In addition, we adopted the PC12 cell line and evaluated the protective effects of the THVF against damage induced by Glu *in vitro*. Meanwhile, western blot assay was conducted to unearth the underlying mechanism and the possible signal pathways involved in the protective effects. Furthermore, we assessed THVF's possible protective effects for *Caenorhabditis elegans* (*C. elegans*) against Glu-induced injury and its potential function in nematode physiological activity.

2. Materials and Methods

2.1. Extraction and Purification of THVF. *T. hemsleyanum* vines were first washed, dried, smashed into powder, and extracted with 80% ethanol at 45°C for 90 min by ultrasonication (with the ratio of material and solution in 1:5). The above extraction produce was repeated three times. Then, the filtered fluid was collected and settled at 4°C overnight. On the second day, the filtrate was centrifuged at 4000 r/min for 10 min to gain the supernatants. Then, the supernatants were evaporated to concentrate under reduced pressure at 45°C, the concentrations were later

centrifuged at 10000 r/min, and then the supernatants were loaded onto an equilibrated AB-8macroporous resin column ($\varnothing 3.2 \times 60$ cm) for further purification. Finally, the eluted fluid was evaporated and lyophilized and later stored at -80°C for further research.

2.2. Identification of THVF. An Ultra Performance Liquid Chromatography (UPLC) system (Waters, Milford, MA, USA) equipped with a triple-Time-of-Flight mass spectrometry (TOF/MS) system (AB SCIEX, Triple TOF 5600+, Framingham, MA, USA) on a Promosil C18 column (4.6 mm \times 250 mm, 5 μ m) was used to identify flavonoid compounds. The ingredients of the mobile phase are acetonitrile (A) and 0.1% aqueous formic acid (B). The linear gradient of phase B was 0–1 min (95%), 1–21 min (95–85%), 21–46 min (85–75%), 46–56 min (75–95%), and 56–60 min (95%). The flow rate was 0.8 mL/min, and the injection amount was 5 μ L. The mass spectrometry was operated in a negative ion mode at a temperature of 550°C, and the source voltage was 4.5 kV. Ions were recorded from *m/z* 100–1500, and the wavelength for the ultraviolet (UV) detector was set as 280 nm.

2.3. Cell Culture and Treatments. PC12 cell line was obtained from Shanghai Institute of Cell Biology (Shanghai, China) and cultured in Dulbecco's modified Eagle's medium (DMEM) supplemented with 10% fetal bovine serum (FBS) and 1% penicillin-streptomycin solution in an incubator with 5% CO₂ at 37°C. THVF powder was always freshly dissolved in DMEM with 10% FBS before use. After being cultured for 24 h, the cells were washed with phosphate-buffered saline (PBS) twice and then pretreated with different concentrations of THVF for another 24 hours. Later, Glu (20 mM) was added for 24 h in the absence/presence of different concentrations of THVF.

2.4. Cell Viability Assays. The assays of cell viability were carried out according to our previous protocol [21]. PC12 cells were seeded onto a 96-well plate, and 3-(4,5-dimethyl-2-thiazolyl)-2,5-diphenyl-2-H-tetrazolium bromide (MTT) diluted with serum-free DMEM at a final concentration of 0.5 mg/mL was added to each well after different treatments. After 4 h of incubation at 37°C, the formazan precipitate was dissolved in 150 μ L of dimethyl sulfoxide (DMSO) and shook for 15 minutes and the absorbance was measured at 570 nm with a spectrophotometer. The viability of the untreated group was regarded as 100%, and each experiment was repeated at least three times.

2.5. Fluorescent Probes Staining for PC12 Cells. After cell treatment, serum-free DMEM, respectively, containing 6 kinds of fluorescent probes were applied, including 2,7-dichlorofluorescein diacetate (DCFH-DA), DHE, apha-thalene-2,3-dicarboxaldehyde (NDA), Rhodamine 123, 10-N nonyl acridine orange (NAO), and Hoechst 33258. Cells were washed twice in PBS buffer after treatments and incubated in free-serum DMEM containing the probe at 37°C for 30 min. Then, cells were washed three times with PBS buffer and detected on a fluorescence microscope (Nikon) with different

filters at identical acquisition settings. Image-Pro Plus 6.0 software was adopted to analyze the densitometry.

2.6. Determination of the Level of SOD, MDA, and GSH. Cells were treated with different treatments, after washing with PBS buffer twice, 500 μ L WB/IP cell lysis buffer was added, and cells were scratched and collected. An ultrasonic shredder and centrifuge (Sigma, USA) were used, and the supernatants were collected for further assay. SOD, MDA, and GSH contents were determined with assay kits purchased from Beyotime Biotechnology (Jiangsu, China).

2.7. Western Blot. Total protein of cells was prepared using the WB/IP lysis buffer (Beyotime Biotechnology, Jiangsu, China). Equal amounts of protein were subjected to sodium dodecyl sulfate-polyacrylamide gel electrophoresis (SDS-PAGE) and transferred to polyvinylidene fluoride (PVDF) membranes. Membranes were probed with primary antibodies, and primary antibodies against p-p38 mitogen-activated protein kinase (MAPK), p38 MAPK, p-JNK, c-Jun N-terminal kinase JNK, and β -actin were purchased from Abcam (Shanghai, China). They were detected with horseradish-peroxidase-conjugated secondary antibodies using the enhanced chemiluminescence (ECL) detection system. β -Actin was used as a loading control, and ImageJ software was used to analyze densitometry.

2.8. C. Elegans Strains and Treatment. *C. elegans* bristol N2 (wild-type) was provided by Dr. Du (Zhejiang University, China). The mutants were maintained at 20°C on a standard nematode growth medium (NGM) with *E. coli* OP50 as food resources. To collect eggs, adult animals on NGM were dissolved in bleaching solution. Then, the eggs were transferred into a new plate for hatching and synchronized at the same period.

Synchronized L3 stage *C. elegans* were collected and transferred to NGM containing THVF of different concentrations (2.5, 5, and 10 μ g/mL). After 24-hour treatments, 20 mM of glutamate was added while the concentration of TVE kept the same as before.

2.9. Determination of Survival Rate, Body Length, and Body Width. The survival rate assays were performed in the 24-well plates. A total of 40 young nematodes were raised in each well with culture medium (NaCl 3.1 g/L, KCl 2.4 g/L, cholesterol 1 mg/L), and *E. coli* OP50 was added for food supply. 0, 2.5, 5, and 10 μ g/mL THVF were added into medium, respectively. After treating for 24 h, 20 mM Glu was later added for another 24 h. Survival rate was defined as survival rate (%) = the living worm numbers after treatment/total worm numbers before treatment * 100%.

The survival rate in the control group was regarded as 100% when calculated. Meanwhile, the photos of *C. elegans* were captured by a microscope and animals' body length and body width were measured by Auto CAD.

2.10. Locomotion Behavior Assay. Head thrash and body bend assays were used to evaluate locomotion behavior ability of nematodes. Once, head thrash was defined as a change in the direction of bending in the mid body which was

counted for 1 min. A body bend was defined as a change in the direction of the part of nematodes corresponding to the posterior bulb of the pharynx along the y -axis, assuming that the long axis of the body was the x -axis ($n = 30$ per replicate; three replicates per group).

2.11. Visualization of ROS, Superoxide, and GSH. To measure the level of ROS, superoxide, and GSH, three fluorescence probes (DCFH-DA, DHE, and NDA) were added, respectively. Images of animals were obtained through a fluorescence microscope.

2.12. Statistical Analysis. Data were expressed as mean \pm standard deviations (SDs) from at least three independent experiments. Significant differences were determined by one-way analysis of variance (ANOVA) followed by the multiple comparison at $p < 0.05$. Significant differences were all analyzed using SPSS. Densitometry analyses were performed using Image-Pro Plus 6.0 software.

3. Results

3.1. The Main Compounds of THVF. UPLC-TOF/MS results showed that THVF was composed of four main compounds; we numbered these four compounds as peak 1, 2, 3, and 4 (Figure 1(a)). As Figure 1(b) illustrated, peak 1 with a molecular ion at m/z 191.0506 [quinic acid-H]⁻ was identified as C₁₆H₁₈O₉, while a series of fragments of m/z 191.0561, 179.0345, 161.0242, 127.0403, and 85.0315 appeared in peak 2 secondary mass spectrum (Figure 1(c)). According to TOF/MS results and previous studies, peaks 1 and 2 were deduced as 3-caffeoylquinic acid and 5-caffeoylquinic acid [21, 25]. Peak 3 with a retention time at 33.923 min and fragment at m/z 301 [M-H-146-162]⁻ was identified as quercetin-3-O-rutinoside. Furthermore, the relative molecular mass of peak 4 was 594, and a fragment of m/z 309 was lost at m/z 285 [M-H-308]⁻ that could correspond to the loss of one rutinoside and peak 7 could be kaempferol-3-O-rutinoside. Therefore, it could be deduced that THVF is consisted of 3-caffeoylquinic acid, 5-caffeoylquinic acid, quercetin-3-O-rutinoside, and kaempferol-3-O-rutinoside.

3.2. THVF Alleviated Oxidative Stress Caused by Glu. According to the results of MTT assay (Figure 1(f)), we found that the concentration range of 0.78–25 μ g/mL showed no toxicity to PC12 cells. Thus, we choose 2.5, 5, 10, and 20 μ g/mL of THVF for further study. DNA damage is a key feature of cytotoxicity [26]. Therefore, Hoechst 33258, a specific DNA fluorescence probe, was adopted to assess nuclear fragmentation. As shown in Figure 2(a), the number of high light blue dots was markedly elevated after Glu stimulation while THVF treatments decreased such light dots at a dose-related manner.

Besides genotoxicity, Glu further caused intracellular redox disturbance, resulting in overproduction of ROS [27]. Since plant flavones were regarded as a potent free radical scavenger both *in vitro* and *in vivo* [28], we tested the intracellular ROS level in the presence or absence of THVF by DCFH-DA, a specific ROS fluorescence probe. An enhanced DCF fluorescence intensity was observed in Glu-treated cells

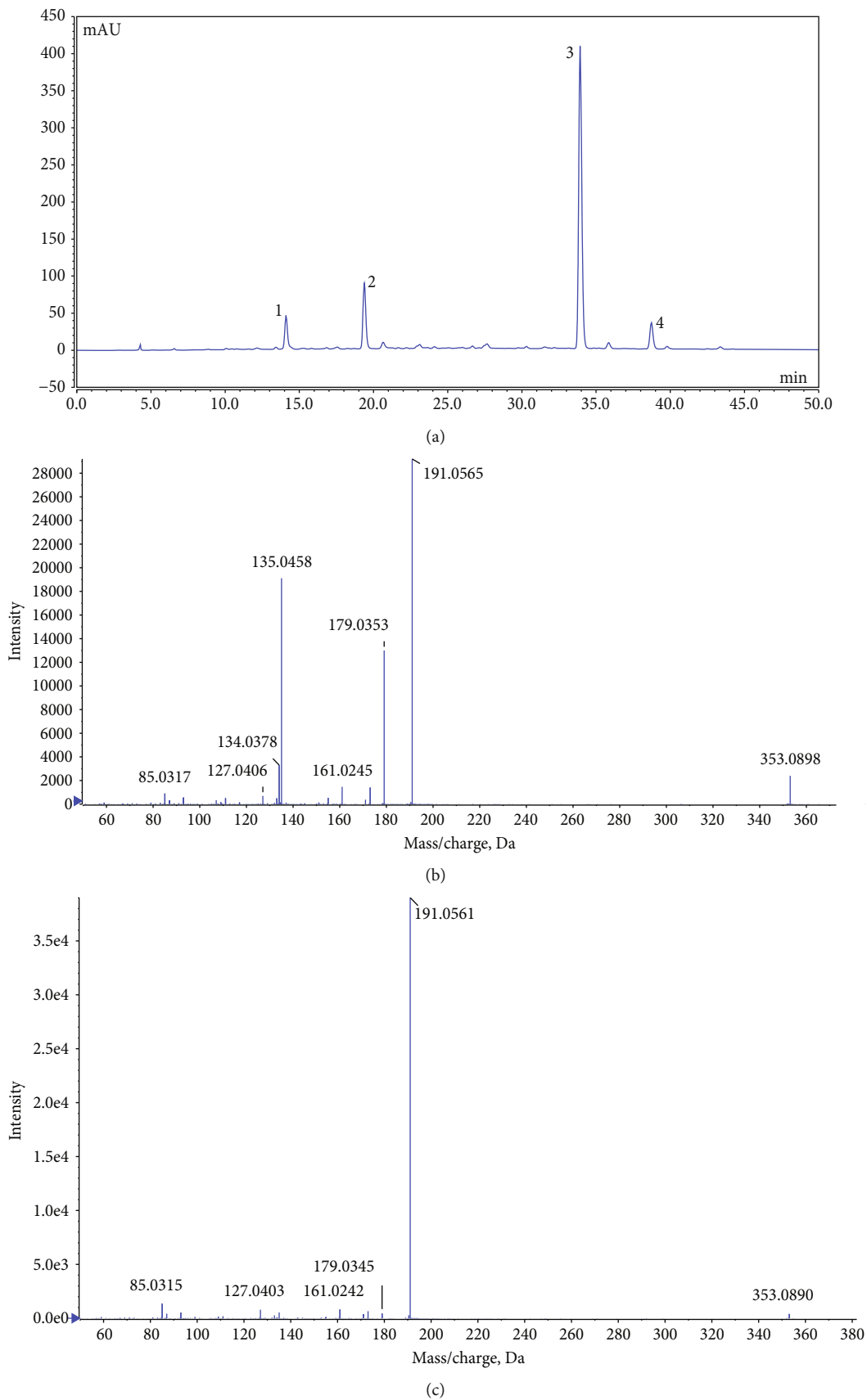


FIGURE 1: Continued.

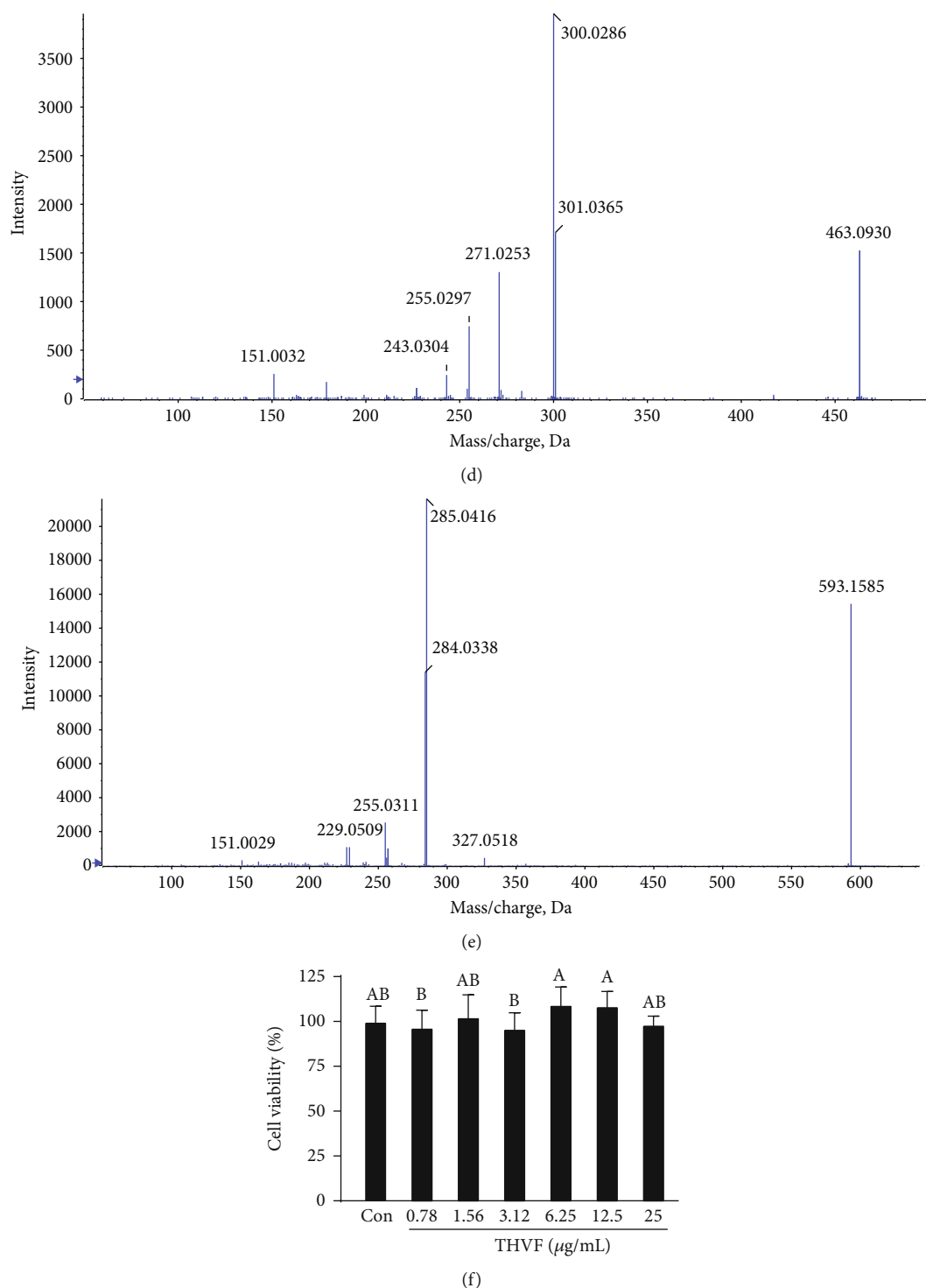


FIGURE 1: HPLC elution profile of compounds in THVF and effects of THVF on cytotoxicity in PC12 cells. (a) The liquid chromatography profile of THVF. The peak numbers were labeled according to the retention times. (b) MS/MS information for peak 1. (c) MS/MS information for peak 2. (d) MS/MS information for peak 3. (e) MS/MS information for peak 4. (f) PC12 cell viability was measured by the MTT method after treated with THVF at different concentrations for 24 h ($n = 6$).

compared with the control group (Figures 2(a) and 2(b)). Intriguingly, 10 and 20 $\mu\text{g/mL}$ THVF significantly declined the ROS level, with the DCF fluorescence intensity decreased to 0.18 and 0.15, respectively. Meanwhile, DHE, a unique probe of intracellular superoxide anion radicals,

was further used to analyze O_2^- contents. Similar findings were got, Glu significantly raised the mean DHE fluorescence intensity of PC12 cells (Figures 2(a) and 2(b)). In contrast, the intervention of THVF helped scavenging the overproduced O_2^- with the DHE fluorescence intensity

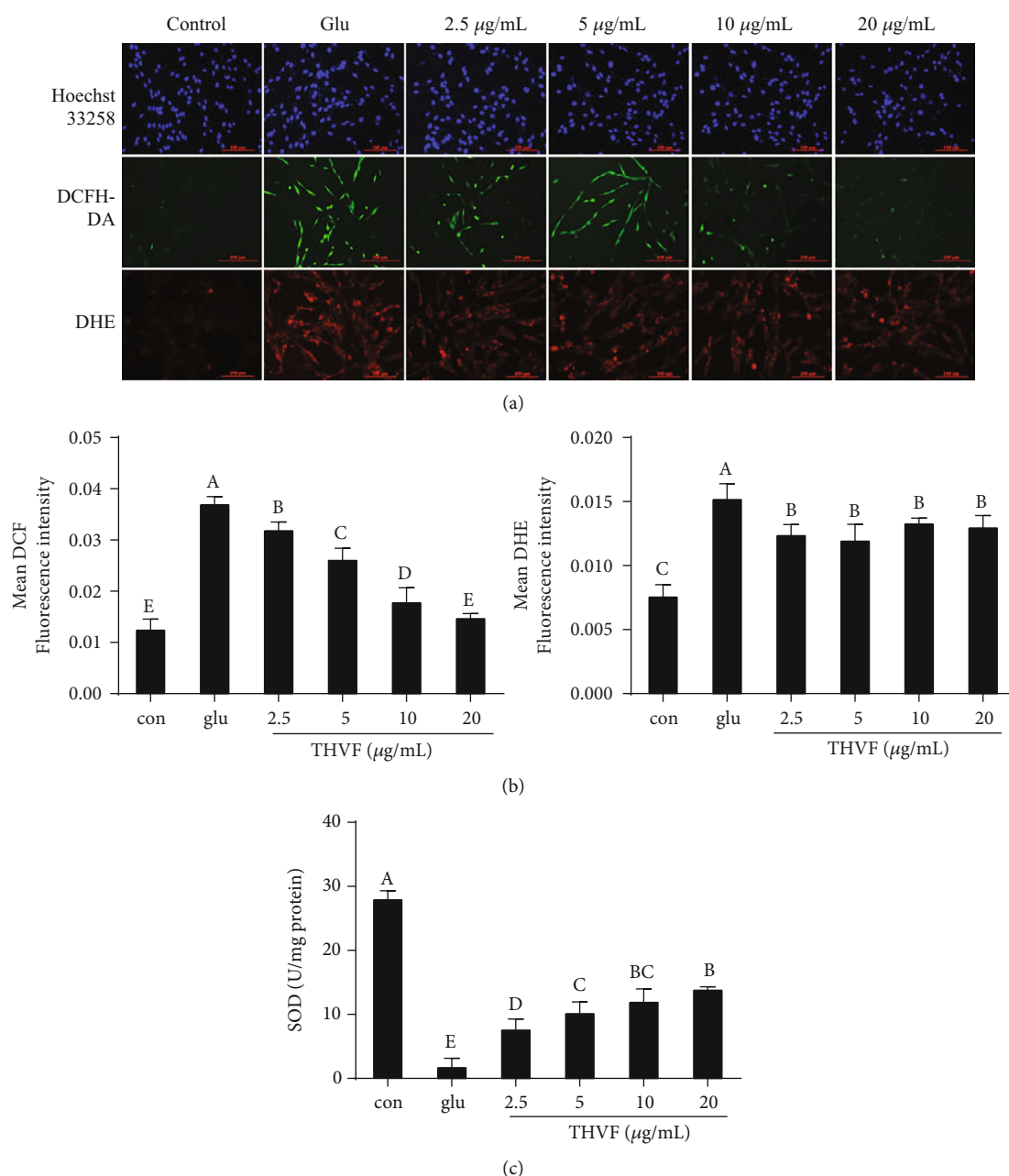


FIGURE 2: Effects of THVF on Glu-induced oxidative damage in PC12 cells ($n = 3$). (a) Hoechst 33258, DCFH-DA, DHE staining for genotoxicity, ROS, and O_2^- . (b) The quantitative data of panel DCFH-DA and DHE. (c) SOD activity of PC12 cells with or without Glu and THVF treatments. THVF-treated cells were inoculated in different concentrations of THVF for 24 hours, and then, 20 mM Glu was added for a total of 24 hours. Cells without Glu and THVF were used as negative control group. Cells treated with Glu alone were used as a glu group. Images were captured with a fluorescence microscope in the same settings. All the fluorescence images were quantified in the whole field with the background removed and represented by normalized fluorescence (y-axes) via Image-Pro Plus 6.0 ($n = 3$). Significance analysis was carried out according to the one-way ANOVA test, and different letters in figures mean statistically significant differences among the groups (a, b, c, etc., were labeled from large to small and once columns containing a same word means statistically insignificant, otherwise means statistically significant, $p < 0.05$).

declined. Superoxide dismutase (SOD) is an antioxidant metalloenzyme that specifically acts as a disproportionation catalyst to suppress superoxide anion radical generation [29]. As Figure 2(c) demonstrated, Glu severely inhibited activity of SOD in PC12 cells. Fortunately, THVF reversed this situation and 20 $\mu\text{g/mL}$ THVF could even recover the

SOD activity similar to control. These dates jointly revealed the protective effect of THVF under Glu-induced toxicity.

3.3. THVF Relieved Mitochondrial Dysfunction Induced by Glu. ROS is often regarded as a by-product of mitochondrial dysfunction [30], and mitochondrial dysfunction could

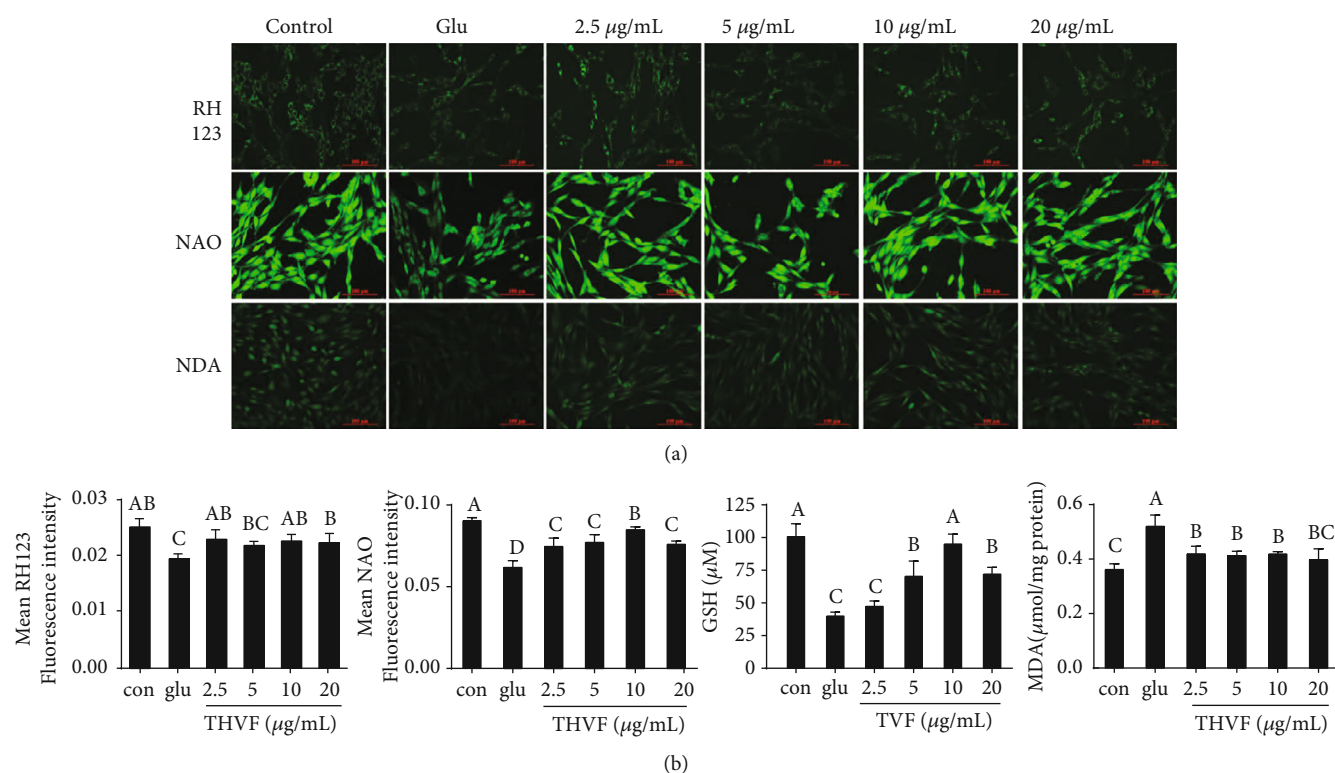


FIGURE 3: Effect of THVF on Glu-induced mitochondrial dysfunction in PC12 cells ($n = 3$). (a) Mitochondrial membrane potential, mitochondrial membrane lipid peroxidation, and GSH alterations of PC12 cells in the presence of Glu and THVF under different treatments and were incubated with RH123, NAO, and NDA probes. (b) The quantitative data of panel (a). Images were captured with a fluorescence microscope in the same settings. All the fluorescence images were quantified in the whole field with the background removed and represented by normalized fluorescence (y -axes) via Image-Pro Plus 6.0 ($n = 3$). Significance analysis was carried out according to one-way ANOVA test and different letters in figures mean statistically significant differences among the groups (a, b, c, etc., were labeled from large to small and once columns containing a same word means statistically insignificant, otherwise means statistically significant, $p < 0.05$).

further accelerate the progression of various diseases, such as atherosclerosis, diabetes, Alzheimer's disease, and Parkinson's disease [31]. Based on these findings, we suspected that THVF might provide a defense effect to the toxicity via recovering mitochondrial function. RH123 fluorescence probe is specific for mitochondrial membrane potential (MMP) detection and NAO is for mitochondrial membrane lipid peroxidation (MMLP), respectively. As Figure 3(a) illustrated, a Rh123 fluorescence intensity decline could be observed with the stimulation of Glu, suggesting the decreased MMP, which is usually regarded as prerequisite and a landmark event in early apoptosis. Similarly, the NAO fluorescence intensity was markedly suppressed by Glu, indicating the disturbed MMLP. However, after THVF treatments, NAO intensity increased compared with Glu-treated cells. Malondialdehyde (MDA) is a crucial product of MMLP, and its production can aggravate damage and leading to aging and resistance physiology [32]. Consistent with previous results, Glu stimulation triggered MDA production and accumulation in PC12 cells while 2.5 µg/mL was sufficient to decrease intracellular MDA content. Mitochondrial dysfunction could further facilitate consumption of glutathione (GSH), and NDA fluorescence intensity reduction was found after Glu stimulation. Conversely, THVF treatments increased intensity significantly, suggest-

ing the alleviation of mitochondrial damage and enhancement of antioxidative ability. Based on these results, we believe THVF exerted a beneficial effect against Glu-induced mitochondrial dysfunction.

3.4. THVF Promoted Cell Proliferation Inhibited by Glu. Besides genotoxicity, ROS generation, and mitochondrial dysfunction, Glu also directly induce PC12 cells apoptosis. B-cell lymphoma-2 (Bcl-2) protein family is closely related to apoptosis [33]. As Figure 4(a) showed, Glu upregulated the Bax expression and suppressed the protein level of Bcl-2, which manifested the apoptotic state of PC12 cells. Besides, the production level of caspase-9 was also increased to 3-fold of control. However, we found THVF obviously down-regulated expressions of Bax, caspase-9, and up-regulated Bcl-2 levels at a dose-dependent manner. PCNA plays a crucial role in cell proliferation and regulating cell cycle [34]. Consists with previous results, Glu significantly inhibited the expression of PCNA, indicating the damage of PC12 cell proliferation caused by Glu. On the contrary, THVF reversed such inhibition and up-regulated PCNA level to 2 times of control. These results suggested that THVF reversed apoptosis induced by Glu and facilitated cell proliferation.

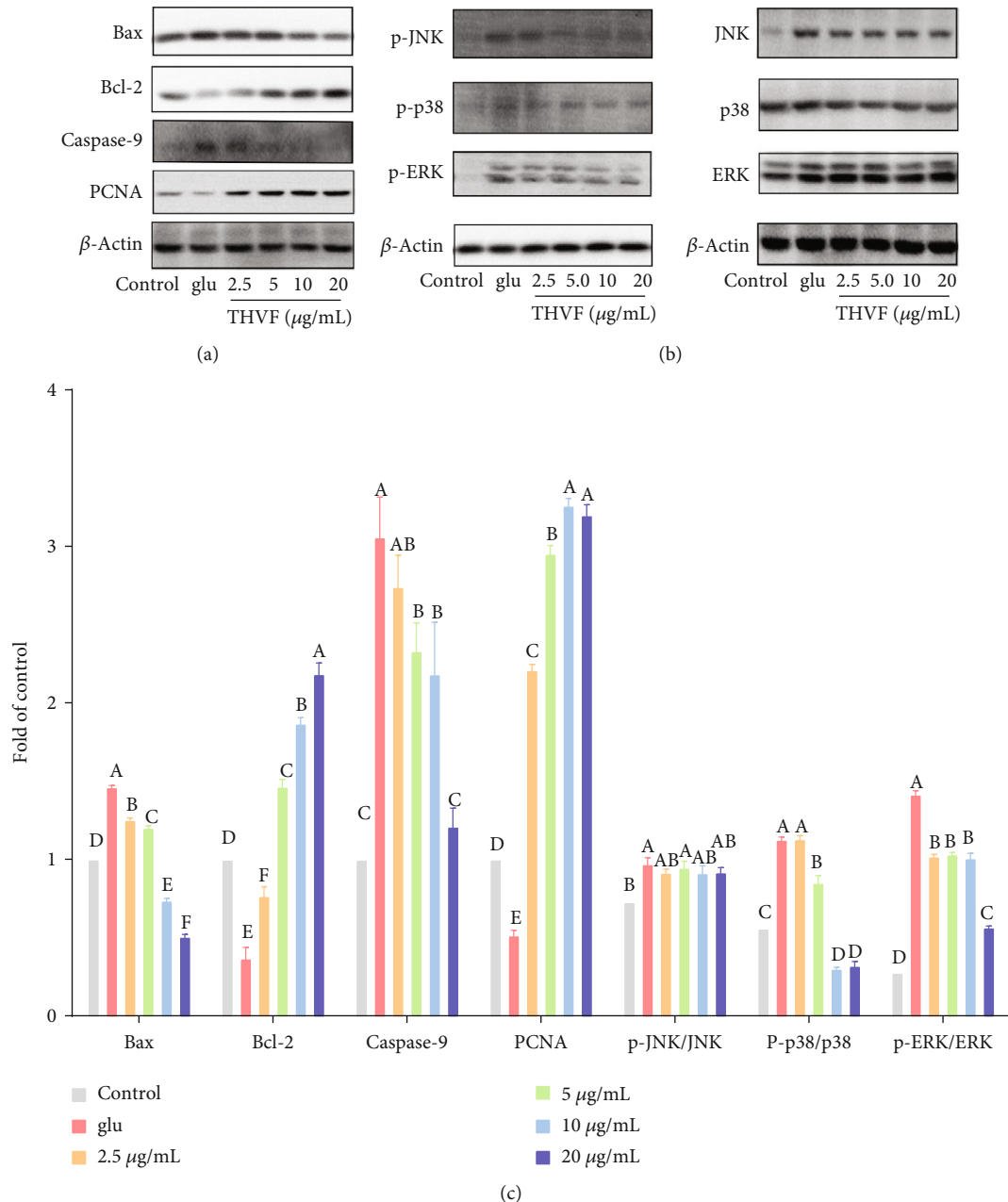


FIGURE 4: THVF treatment altered expressions of proteins in PC12 cells. (a) Western blot bands of Bax, Bcl-2, caspase-9, PCNA, and β -actin ($n = 3$). (b) Western blot bands of MAPKs. p-JNK, p-p38, and p-ERK represent phosphorylation of JNK, p38, and ERK. (c) Relative expressions of Bax, Bcl-2, caspase-9, PCNA, p-JNK, p-p38, p-ERK, JNK, p38, and ERK. The images were quantified by ImageJ software, the intensity of bands was corrected by β -actin ($n = 3$), and vertical lines in the histogram represent SDs of three replicates. Significance analysis was carried out according to the one-way ANOVA test, and different letters mean statistically significant differences among the groups (a, b, c, etc., were labeled from large to small and once columns containing a same word means statistically insignificant, otherwise means statistically significant, $p < 0.05$).

3.5. The Protective Effect of THVF Involved in MAPK Pathways. As an important transmitter of signals from the cell surface to the interior of the nucleus, MAPKs can be activated by different extracellular stimuli such as cytokines, hormones, and cellular stress [35]. Figure 4(b) showed that with the stimulation of Glu, the phosphorylation of JNK, ERK, and p38 was upregulated. However, after THVF treatments, downregulation of phospho-p38 and phospho-ERK was observed. Meanwhile, though

THVF had both inhibited the expression level of total JNK and p-JNK, the ratio of p-JNK/JNK had not changed compared to Glu-induced cells. Based on these results, we deduced that THVF protect PC12 cells from toxicity via ERK/p38 pathways.

3.6. THVF Recovered the Locomotory Ability of *C. elegans*. With short lifespan and low cost, *C. elegans* is regarded as an ideal *in vivo* model to study toxicity [36]. As shown

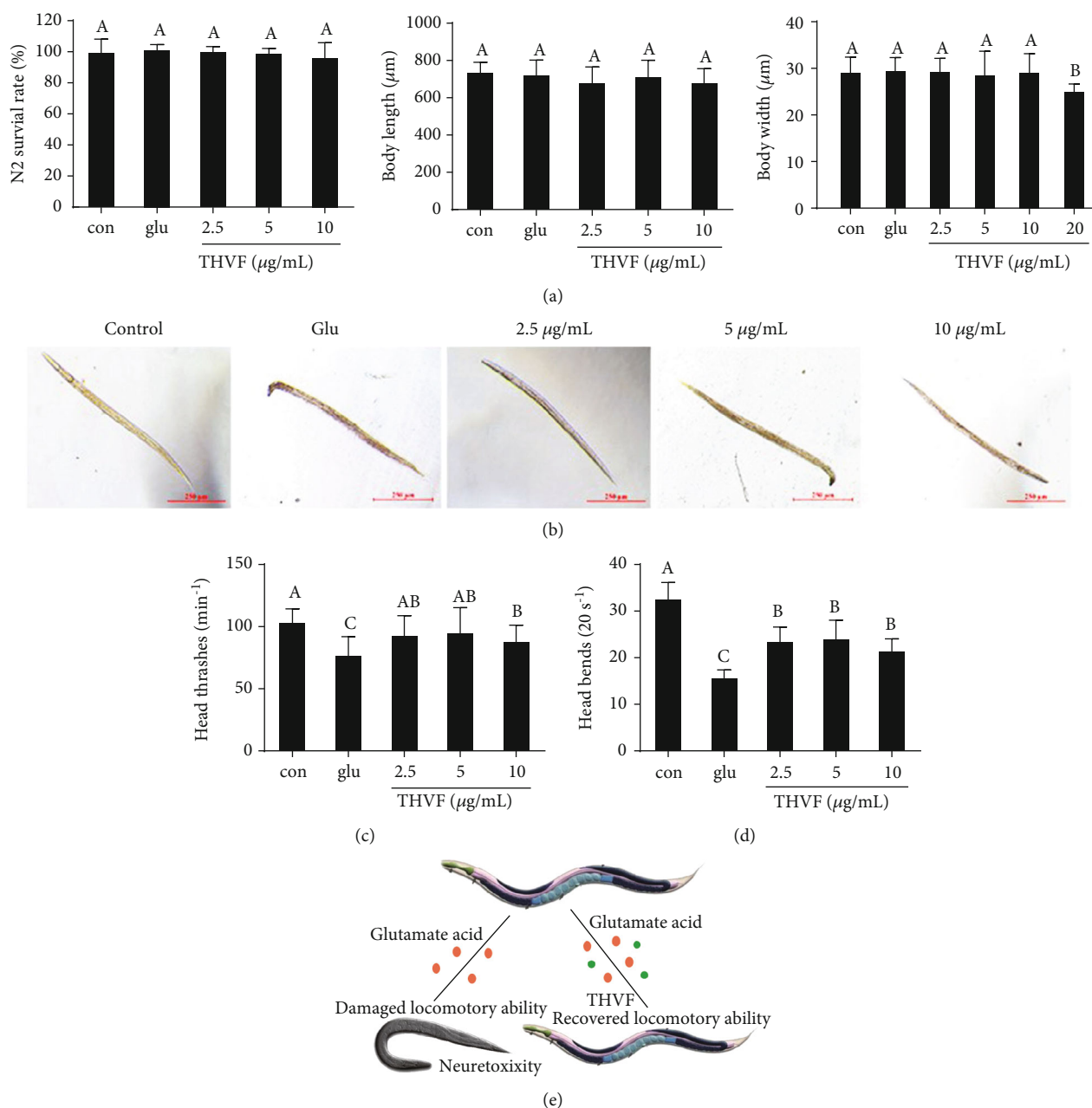


FIGURE 5: Effect of THVF on Glu-induced toxicity in *C. elegans* ($n = 30$). (a) Survival rate, body length, and body width of different groups in N2. (b) Representative photographs of *C. elegans* with different treatments. (c) Head thrashes of different groups in N2. (d) Body-bending frequency of different groups in N2. (e) Scheme illustration of Glu and THVF on nematode locomotory activity. Significance analysis was carried out according to the one-way ANOVA test, and different letters show statistically significant differences among the groups ($p < 0.05$).

in Figures 5(a) and 5(b), both Glu and THVF had not affected the survival rate, body length, and body width of nematode. However, Glu stimulation caused severe damage to nematodes' locomotory ability. Our results showed significant decreases in body bends and head thrashes of *C. elegans* after exposure to Glu (Figures 5(c) and 5(d)), implying the neurotoxicity of Glu, while THVF partly recovered the locomotory abilities of nematodes. Based on these results, our results demonstrated that Glu could induce considerably severe locomotor defects and THVF

was capable to protect nematodes from Glu-induced neurotoxicity (Figure 5(e)).

3.7. THVF Protected *C. elegans* from Glu-Induced Oxidative Stress. In *in vitro* study, Glu induced oxidative toxicity to PC12 cells and THVF effectively alleviated oxidative stress. To confirm whether THVF could help prevent from oxidative damage *in vivo*, we used DCF, DHE, and NDA probes to measure intracellular ROS, O_2^- , and GSH depletion in *C. elegans*, respectively. Figure 6 demonstrated that the

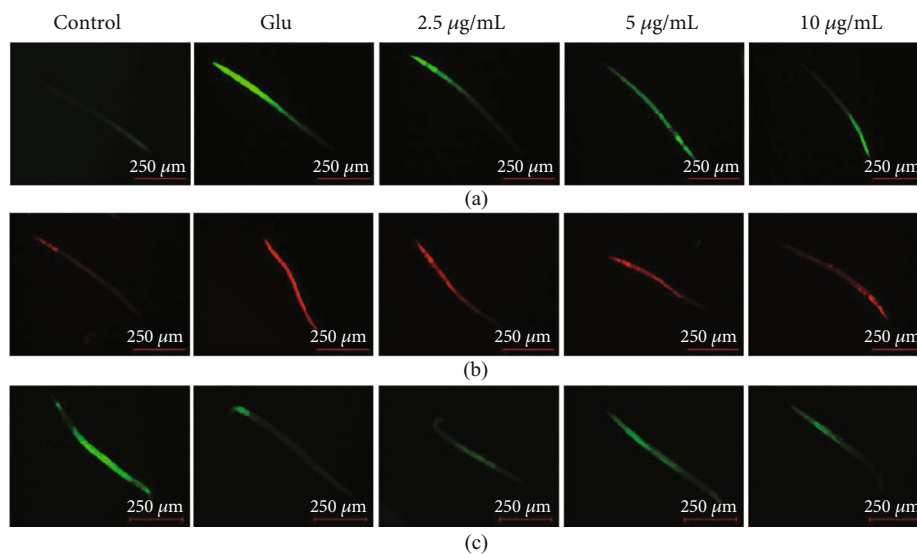


FIGURE 6: Fluorescence staining for *C. elegans* ($n = 30$). (a) DCFH-DA staining for ROS alteration. (b) DHE staining for O_2^- alteration. (c) NDA staining for GSH contents. Images were captured with a fluorescence microscope in the same settings ($n = 6$).

treatment of Glu remarkably increased the mean DCF fluorescence intensity whereas the addition of THVF restored the mean DCF fluorescence intensity as expected at a dose-related manner. Moreover, Glu enhanced the level of O_2^- and facilitated the GSH depletion in nematodes. On the contrary, THVF intervention suppressed the generation of O_2^- and restrained GSH depletion. These results above suggested that THVF could attenuate Glu-induced oxidative damage in *C. elegans*.

4. Discussion

The Chinese have used certain seaweeds to enhance the flavor of food for some 2,000 years. In 1908, the flavor-enhancing agent was identified as glutamic acid [37]. Nowadays, Glu has been applied to a large amount of industrial production with its various applications such as flavor enhancer, wrinkles reducer, energy supplier, and neurotherapeutic agent. However, the toxicity especially neurotoxicity of Glu has been continuously uncovered recently. Many studies have revealed that natural products are able to help alleviate toxicity and protect from outer stimulation. TH is a traditional Chinese herb and food with various confirmed bioactive functions, while TH vine is usually regarded useless and often discarded as a by-product, resulting in a waste of source. We extracted and purified the flavones of TH and use UPLC-TOF/MS to characterized the main compounds of THVF. Results showed that THVF was composed of 3-caffeoylquinic acid, 5-caffeoylquinic acid, quercetin-3-O-rutinoside, and kaempferol-3-O-rutinoside.

With extreme versatility for pharmacological manipulation, ease of culture, and the large amount of background knowledge on their proliferation and neuro characterization, rat pheochromocytoma (PC12) cells have been widely used as a model for neural research [38]. Glu caused severe genotoxicity to PC12, hereby triggered enhanced ROS generation and overproduction of O_2^- , which were by-products of mito-

chondrial dysfunction induced by Glu. Additionally, Glu inhibited the SOD enzyme activity and then increased the MDA accumulation as results. Conversely, THVF attenuated the Glu-induced toxicity by alleviating the genotoxicity, relieving oxidative stress, and recovering mitochondrial functions. It is implying that cell death in central nervous system irregularly may play a part in an etiology of cancer, AIDS, autoimmune diseases, and degenerative diseases such as Alzheimer's disease (AD), amyotrophic lateral sclerosis (ALS), and Huntington's disease. Similarly, PC12 cell proliferation was inhibited by Glu with down-regulation of PCNA and Bcl-2, as well as up-regulation of Bax and caspase-9, suggesting the apoptosis of cells. As expected, THVF recovered the cell proliferate ability and enhanced the expression levels of PCNA, Bcl-2.

Mitogen-activated protein kinase (MAPK), as an important transmitter of signal transmission from the cell surface to the interior of the nucleus, plays a key role in stress response [35]. Glu markedly activated the phosphorylation of p38, JNK, and ERK. Nevertheless, down-regulation of p38 phosphorylation was found in THVF treated cells. Considering p38 MAPK is vital in immune response to stress and cell survival [39], THVF can inactivate, at least partly, the p38 MAPK pathway. Besides, THVF suppressed the expression of Glu-induced ERK over-phosphorylation. Previous studies have reported that ERKs, as a downstream protein of various growth factors (EGF, NGF, PDGF), regulate cell proliferation, differentiation, and survival. It acts like a receptor of signals from growth factors, mitogens, and environmental stimuli and then regulates nuclear transcription factors through the ERK signal cascade [40]. Thus, THVF might help protect PC12 cells from Glu-induced toxicity by suppressing over-phosphorylation of ERK and p38.

It has been proved that neurotransmitters and their metabolism, vesicle circulation, and synaptic transmission are highly conserved, and all 302 neurons of the nematode have been well studied, which makes *C. elegans* an ideal

model to learn neurotoxicity and behavior *in vivo* [41]. Locomotor behaviors require the control of neural circuits [42]. Our results implied that Glu toxicity might be involved in the disruption of motor control function or appropriate synaptic contacts between neurons and muscle cells. As *C. elegans* lacks a functional blood-brain barrier, Glu could quickly diffuse into the nervous system and directly produce neurotoxic actions, resulting in damaged head thrashes and body bends. Fortunately, here THVF turned to be a neuroprotective agent and recovered the locomotory ability of nematodes. Consistent with *in vitro* results, Glu elevated the intracellular ROS, O₂⁻ generation, and GSH depletion in nematodes and THVF prevented larvae from Glu-toxicity. However, it is unclear whether MAPK pathways are also involved in the THVF-treated nematodes, and further research is needed to confirm the inner mechanism in *C. elegans* level.

5. Conclusion

In this study, we focus on Glu neurotoxicity rather than its wide applications and well-known protective effects. As results illustrated, Glu caused damage to PC12 cells and *C. elegans* while THVF, flavones extracted, and purified from TH vine was able to protect Glu-induced toxicity via MAPK pathways. These data provide a novel insight and raise worthwhile questions about the Glu-accompanied side-toxicity and THVF potential neuroprotective effects both *in vitro* and *in vivo*, as well as MAPK pathways' role in neurotoxicity.

Data Availability

The data used to support the findings of this study are available from the corresponding author upon request.

Conflicts of Interest

The authors have declared no conflict of interest.

Authors' Contributions

Qiang Chu and Yonglu Li contributed equally to this work.

Acknowledgments

This work was supported by the Science and Technology Department of Zhejiang Province (No. 2018C02045) and Shanghai Zhengyue Enterprise Management Co., Ltd.

References

- [1] P. J. Reeds, "Dispensable and indispensable amino acids for humans," *The Journal of Nutrition*, vol. 130, no. 7, pp. 1835S–1840S, 2000.
- [2] S. Jinap and P. Hajeb, "Glutamate. Its applications in food and contribution to health," *Appetite*, vol. 55, no. 1, pp. 1–10, 2010.
- [3] T. Populin, S. Moret, S. Truant, and L. S. Conte, "A survey on the presence of free glutamic acid in foodstuffs, with and without added monosodium glutamate," *Food Chemistry*, vol. 104, no. 4, pp. 1712–1717, 2007.
- [4] A. N. Williams and K. M. Woessner, "Monosodium glutamate 'allergy': menace or myth?," *Clinical and Experimental Allergy*, vol. 39, no. 5, pp. 640–646, 2009.
- [5] O. P. Ottersen, Y. Takumi, A. Matsubara, A. S. Landsend, J. H. Laake, and S. Usami, "Molecular organization of a type of peripheral glutamate synapse: the afferent synapses of hair cells in the inner ear," *Progress in Neurobiology*, vol. 54, no. 2, pp. 127–148, 1998.
- [6] P. Pichler and L. Lagnado, "The transfer characteristics of hair cells encoding mechanical stimuli in the lateral line of zebrafish," *The Journal of Neuroscience*, vol. 39, no. 1, pp. 112–124, 2019.
- [7] A. Ogunleye, A. Bhat, V. U. Irorere, D. Hill, C. Williams, and I. Radecka, "Poly-γ-glutamic acid: production, properties and applications," *Microbiology*, vol. 161, no. 1, pp. 1–17, 2015.
- [8] H. A. Krebs, "Metabolism of amino-acids: the synthesis of glutamine from glutamic acid and ammonia, and the enzymic hydrolysis of glutamine in animal tissues," *The Biochemical Journal*, vol. 29, no. 8, pp. 1951–1969, 1935.
- [9] J. S. Najarian and H. A. Harper, "Comparative effect of arginine and monosodium glutamate on blood ammonia," *Proceedings of the Society for Experimental Biology and Medicine*, vol. 92, no. 3, pp. 560–563, 1956.
- [10] K. Krnjevic, "Glutamate and gamma-aminobutyric acid in brain," *Nature*, vol. 228, no. 5267, pp. 119–124, 1970.
- [11] M. Kobayashi, C. Benakis, C. Anderson et al., "AGO CLIP reveals an activated network for acute regulation of brain glutamate homeostasis in ischemic stroke," *Cell Reports*, vol. 28, no. 4, pp. 979–991.e6, 2019.
- [12] A. da Silva-Candal, A. Pérez-Díaz, M. Santamaría et al., "Clinical validation of blood/brain glutamate grabbing in acute ischemic stroke," *Annals of Neurology*, vol. 84, no. 2, pp. 260–273, 2018.
- [13] Z. Zhou, G. L. Austin, L. Young, L. A. Johnson, and R. Sun, "Mitochondrial metabolism in major neurological diseases," *Cells*, vol. 7, no. 12, p. 229, 2018.
- [14] S. Bleich, K. Romer, J. Wiltfang, and J. Kornhuber, "Glutamate and the glutamate receptor system: a target for drug action," *International Journal of Geriatric Psychiatry*, vol. 18, Supplement 1, pp. S33–S40, 2003.
- [15] M. T. Islam, "Oxidative stress and mitochondrial dysfunction-linked neurodegenerative disorders," *Neurological Research*, vol. 39, no. 1, pp. 73–82, 2017.
- [16] J. T. Coyle and P. Puttfarcken, "Oxidative stress, glutamate, and neurodegenerative disorders," *Science*, vol. 262, no. 5134, pp. 689–695, 1993.
- [17] R. D. Randall and S. A. Thayer, "Glutamate-induced calcium transient triggers delayed calcium overload and neurotoxicity in rat hippocampal neurons," *The Journal of Neuroscience*, vol. 12, no. 5, pp. 1882–1895, 1992.
- [18] N. Plotegher, D. Perocheau, R. Ferrazza et al., "Impaired cellular bioenergetics caused by GBA1 depletion sensitizes neurons to calcium overload," *Cell Death & Differentiation*, 2019.
- [19] S. A. Novgorodov, J. R. Voltin, M. A. Gooz, L. Li, J. J. Lemasters, and T. I. Guduz, "Acid sphingomyelinase promotes mitochondrial dysfunction due to glutamate-induced regulated necrosis," *Journal of Lipid Research*, vol. 59, no. 2, pp. 312–329, 2018.

- [20] Y. Yu, M. Shen, Q. Song, and J. Xie, "Biological activities and pharmaceutical applications of polysaccharide from natural resources: a review," *Carbohydrate Polymers*, vol. 183, pp. 91–101, 2018.
- [21] Y. Li, Q. Chu, Y. Liu, X. Ye, Y. Jiang, and X. Zheng, "Radix *Tetragium* flavonoid ameliorates inflammation and prolongs the lifespan of *Caenorhabditis elegans* through JNK, p38 and Nrf2 pathways," *Free Radical Research*, vol. 53, no. 5, pp. 562–573, 2019.
- [22] Q. Chu, R. Jia, W. Chen et al., "Purified *Tetragium hemsleyanum* vines polysaccharide attenuates EC-induced toxicity in Caco-2 cells and *Caenorhabditis elegans* via DAF-16/FOXO pathway," *International Journal of Biological Macromolecules*, 2019.
- [23] Q. Chu, R. Jia, M. Chen et al., "*Tetragium hemsleyanum* tubers polysaccharide ameliorates LPS-induced inflammation in macrophages and *Caenorhabditis elegans*," *International Journal of Biological Macromolecules*, vol. 141, pp. 611–621, 2019.
- [24] X. Chen, L. Tao, Y. Ru et al., "Antibacterial mechanism of *Tetragium hemsleyanum* Diels et Gilg's polysaccharides by metabolomics based on HPLC/MS," *International Journal of Biological Macromolecules*, vol. 140, pp. 206–215, 2019.
- [25] J. Kolniak-Ostek, "Identification and quantification of polyphenolic compounds in ten pear cultivars by UPLC-PDA-Q/TOF-MS," *Journal of Food Composition and Analysis*, vol. 49, pp. 65–77, 2016.
- [26] M. Pagano and C. Faggio, "The use of erythrocyte fragility to assess xenobiotic cytotoxicity," *Cell Biochemistry and Function*, vol. 33, no. 6, pp. 351–355, 2015.
- [27] A. Sharma, "Monosodium glutamate-induced oxidative kidney damage and possible mechanisms: a mini-review," *Journal of Biomedical Science*, vol. 22, no. 1, p. 93, 2015.
- [28] S. H. Nile, Y. S. Keum, A. S. Nile, S. S. Jalde, and R. V. Patel, "Antioxidant, anti-inflammatory, and enzyme inhibitory activity of natural plant flavonoids and their synthesized derivatives," *Journal of Biochemical and Molecular Toxicology*, vol. 32, no. 1, article e22002, 2018.
- [29] S. Signorella, C. Palopoli, and G. Ledesma, "Rationally designed mimics of antioxidant manganoenzymes: role of structural features in the quest for catalysts with catalase and superoxide dismutase activity," *Coordination Chemistry Reviews*, vol. 365, pp. 75–102, 2018.
- [30] J. M. Flynn and S. Melov, "SOD2 in mitochondrial dysfunction and neurodegeneration," *Free Radical Biology & Medicine*, vol. 62, pp. 4–12, 2013.
- [31] T. Jiang, Q. Sun, and S. Chen, "Oxidative stress: a major pathogenesis and potential therapeutic target of antioxidative agents in Parkinson's disease and Alzheimer's disease," *Progress in Neurobiology*, vol. 147, pp. 1–19, 2016.
- [32] S. Feng, H. Cheng, Z. Xu et al., "Thermal stress resistance and aging effects of *Panax notoginseng* polysaccharides on *Caenorhabditis elegans*," *International Journal of Biological Macromolecules*, vol. 81, pp. 188–194, 2015.
- [33] R. J. Youle and A. Strasser, "The BCL-2 protein family: opposing activities that mediate cell death," *Nature Reviews Molecular Cell Biology*, vol. 9, no. 1, pp. 47–59, 2008.
- [34] W. Strzalka and A. Ziemienowicz, "Proliferating cell nuclear antigen (PCNA): a key factor in DNA replication and cell cycle regulation," *Annals of Botany*, vol. 107, no. 7, pp. 1127–1140, 2011.
- [35] B. Su and M. Karin, "Mitogen-activated protein kinase cascades and regulation of gene expression," *Current Opinion in Immunology*, vol. 8, no. 3, pp. 402–411, 1996.
- [36] M. C. Leung, P. L. Williams, A. Benedetto et al., "*Caenorhabditis elegans*: an emerging model in biomedical and environmental toxicology," *Toxicological Sciences*, vol. 106, no. 1, pp. 5–28, 2008.
- [37] A. Samuels, "The toxicity/safety of processed free glutamic acid (MSG): a study in suppression of information," *Accountability in Research*, vol. 6, no. 4, pp. 259–310, 1999.
- [38] R. H. S. Westerink and A. G. Ewing, "The PC12 cell as model for neurosecretion," *Acta Physiologica*, vol. 192, no. 2, pp. 273–285, 2008.
- [39] T. M. Thornton and M. Rincon, "Non-classical p38 map kinase functions: cell cycle checkpoints and survival," *International Journal of Biological Sciences*, vol. 5, no. 1, pp. 44–51, 2009.
- [40] B. Sparta, M. Pargett, M. Minguet, K. Distor, G. Bell, and J. G. Albeck, "Receptor level mechanisms are required for epidermal growth factor (EGF)-stimulated extracellular signal-regulated kinase (ERK) activity pulses," *The Journal of Biological Chemistry*, vol. 290, no. 41, pp. 24784–24792, 2015.
- [41] K. Kamireddy, S. Chinnu, P. S. Priyanka, P. S. Rajini, and P. Giridhar, "Neuroprotective effect of *Decalepis hamiltonii* aqueous root extract and purified 2-hydroxy-4-methoxy benzaldehyde on 6-OHDA induced neurotoxicity in *Caenorhabditis elegans*," *Biomedicine & Pharmacotherapy*, vol. 105, pp. 997–1005, 2018.
- [42] H. Kohsaka, P. A. Guertin, and A. Nose, "Neural circuits underlying fly larval locomotion," *Current Pharmaceutical Design*, vol. 23, no. 12, pp. 1722–1733, 2017.